JGR Space Physics

RESEARCH ARTICLE
10.1029/2020JA028194

Auroral Arcs: The Fracture Theory Revisited

Gerhard Haerendel[1]

[1]Max Planck Institute for Extraterrestrial Physics, Garching, Germany

Supporting Information:
- Supporting Information S1

Correspondence to:
G. Haerendel,
hae@mpe.mpg.de

Citation:
Haerendel, G. (2021). Auroral arcs: The fracture theory revisited. *Journal of Geophysical Research: Space Physics*, *126*, e2020JA028194. https://doi.org/10.1029/2020JA028194

Received 11 MAY 2020
Accepted 25 SEP 2020

Abstract The fracture theory for auroral arcs, developed by the author since 1980, compares the decoupling of the magnetic field from the ionosphere by the auroral acceleration region (AAR) with the breaking of a solid rod. In the latter elastic energy stored by the bending is converted into kinetic energy of the stress release motion. Similarly, magnetic energy stored in sheared magnetic fields is temporarily converted into stress release motions and finally transported as Poynting flux into the AAR. The fracture theory has been especially applied to arcs embedded in the convection of the evening auroral oval. The present study subjects the different steps in the fracture process to a critical analysis in the light of new physical insights. This boils down to a revision of the illustrating cartoon used in the earlier publications, without having affecting the quantitative evaluations. The first revision concerns the height extent of the AAR. It must be largely increased. The second revision introduces a nearly 2-D magnetohydrodynamics (MHD) turbulence into the state of the AAR. This is supported by high-altitude electric field data and leads to new view of auroral rays. The third revision describes the transition from the AAR to the ionosphere as structured by so-called potential fingers, which contain substantial fractions of the total field-parallel potential drop. The most important modification pertains to the average U-shaped potential of a spontaneously propagating AAR. While the leading edge of the auroral current sheet is structured by stress release motions, the reverse flow in the rear section escapes simple interpretation. It is proposed that this flow is driven by a turbulent transport of reversed momentum from front to rear in response to the incompressibility of the magnetic field in the acceleration region. This leads to a revision of the field-aligned currents and wavefield in the rear of the arc.

1. Introduction

The observation that auroral arcs were related with the precipitation of nearly mono-energetic electrons (Evans, 1968; McIlwain, 1960) led to the conclusion that acceleration by field-parallel electric fields were at work. Ackerson and Frank (1972) discovered that the energy-time spectrogram of precipitating electrons in the evening auroral zone had the shape of an "inverted V," that is, the energy increased to a maximum and subsequently decreased as the spacecraft passed through the precipitation band. Decisive was the finding that the transverse electric field was reversing directions through an inverted V structure (Franck & Gurnett, 1971) and the interpretation by Gurnett (1972) that the accelerating field was part of a U-shaped electrostatic potential structure embedded in a strong upward directed electric current. The associated anisotropic distribution of the electron intensities downward along the magnetic field direction confirmed their acceleration by field-parallel electric fields. Haerendel et al. (1976) observed field-parallel acceleration of barium ions injected above an auroral arc, gaining energy of several keV. Mozer et al. (1977) measured spatially confined regions of very strong electric fields at altitudes up to 8,000 km, which frequently had a double structure of converging electric fields. They named them "electrostatic shocks." This was inspired by the model of strongly oblique electrostatic shocks proposed by Swift (1975, 1979). A later survey of the electric fields measured during the same mission (S3-3) revealed that the inverted V structures were less common than single S-shaped potential structures (Mozer et al., 1980). Mizera et al. (1982) showed that the derived potential structure depended strongly on the altitude of the measurement. Further important steps in the exploration of the accelerating potentials were the identifications of upgoing ion beams (Shelley et al., 1976) and of upgoing electron beams (Marklund et al., 1994). The latter were shown to be associated with diverging electric fields in downward current regions. These and other measurements established

firmly the large-scale structure of the auroral acceleration region (AAR) as an electrostatic U- or S-shaped potential distribution.

The other, at least equally important aspect of the auroral electric fields was the nature of the processes sustaining the parallel components. Kindel and Kennel (1971) presented a theoretical model of the generation of anomalous resistivity caused by wave turbulence driven by current-driven instabilities. Kintner et al. (1978) examined plasma waves associated with the potential structures and upward ion beams and found strong correlations with electrostatic hydrogen cyclotron waves. Block (1972) calculated potential drops of tens of kilometer, so-called double layers, maintained by the momentum balance of accelerated and inflowing particles. Another very fruitful approach was the recognition by Knight (1973) and Fridman and Lemaire (1980) that due to the mirror effect there is a relationship between field-parallel potential drop and upward current intensity in a sufficiently dilute collisionless plasma. The discovery of Lyons et al. (1979) that the downward electron energy flux varied as the square of the accelerating potential drop had an important consequence. It suggested the existence of a simple current-voltage relation. This was recognized by Lyons (1980) who derived from the above cited theories a field-parallel conductance governing the relation between an upward field-aligned current and the parallel potential drop. Defining an outer boundary potential and an associated field-aligned current, Lyons (1980) derived the transverse potential in the ionosphere by using a theoretical value of this conductance. Matching the divergence of the Pedersen current with the upward current led to a characteristic transverse scale. Initially interpreted as describing the width of an inverted V, it was later named the magnetospheric-ionospheric (M-I) coupling scale or electrostatic M-I scale. It is typically of the order of a few 100 km. Indeed, inverted Vs cover a wide range of widths, form a few tens of kilometer up to more than 100 km with a maximum of the distribution near 30 km (Partamies et al., 2008). The wider cases, appearing optically as diffuse, weak arcs, often show substructures of tens of kilometer.

It was soon recognized that describing the aurora by electrostatic models was inconsistent with the omnipresent temporal changes. Goertz (1981) investigated Alfvén wave packages launched from rapid changes of the magnetospheric convection pattern as origin of discrete breakup arcs, in particular kinetic Alfvén waves with transverse scales of the order of the electron skin depth. Parallel electric fields in the front and back of the wave package could accelerate electrons to auroral energies. More generally, Lysak (1981) showed that matching the wave impedance of the energy carrying Alfvén wave with the inverse conductance of (Lyons, 1980) determined a scale length appropriate for narrow structured auroral arcs. Lysak and Dum (1983) used a two-dimensional MHD model to calculate multiply reflected Alfvén waves between generator and ionosphere including anomalous resistivity where the parallel current exceeded a critical threshold. They showed that the energy derived from twisting the magnetic field was mostly absorbed in the region of anomalous resistivity and dominantly converted into the energy of runaway electrons. Contrary to the electrostatic models, a current generator was employed in this model. Lysak (1985) generalized the electrodynamic coupling between magnetosphere and ionosphere for current as well as voltage generators.

In the above cited and related work the energy was transported from above explicitly or implicitly as Poynting flux in the Alfvén mode. Although the presence of field-aligned currents was essential, some of the models considered either balanced Alfvén waves or truncated current circuits without identification of the return currents. The author (Haerendel, 1980) took a different approach. He considered the auroral arc as a narrow upward current sheet embedded in a large-scale M-I convection system or as a current circuit of Type 2 according to Boström (1964). The convection of the magnetospheric plasma is seen as driven by forces in the outer magnetosphere (e.g., pressure forces) against the friction with the neutral atmosphere. Forces are transported by magnetic shear stresses toward the ionosphere. The associated quasisteady field-aligned currents close through the ionosphere. While in the quiet convection the field-aligned currents are force-free, the situation can be disturbed in narrow current sheets at heights above the extent of the topside ionosphere, where, primarily owed to the magnetic mirror force acting on the current carrying electrons, some kind of resistance is encountered and parallel electric fields develop. As a consequence, the connection between generator and ionosphere is locally decoupled. Decoupling means that the shear stresses are not transferred to the ionosphere, but transformed into plasma motions along the way to the ionosphere. Magnetic energy is temporarily converted into kinetic energy of flow. This energy is carried from above as Poynting flux into the acceleration region by quasistationary slightly oblique Alfvén waves. These waves

are excited by the AAR propagating into the still stressed magnetic field. Inside the AAR, the near-electrostatic nature of the electric field leads to a U-shaped potential distribution, which expresses the intimate connection between the transverse wavefield and the transverse and parallel electrostatic field components representing the decay of the Poynting flux. This is seen as the essence of auroral arc formation, at least for those embedded in a larger convection system. There is a certain kinship with thee feedback model of Sato (1978) in that the energy invested in the parallel acceleration is derived from the magnetic energy content of a current circuit. However, this circuit consists of adjacent upward and downward currents driven by narrow convection lanes.

In order to visualize the above described process, the author compared the auroral current sheet with a bent elastic rod and the electrostatic decoupling in a region of strong current concentration with the appearance of a fracture in a region of high mechanical stress concentration. Breaking means that the body on either side of the fracture would start moving by releasing the shear stresses and converting the energy into kinetic energy of motion. In the magnetic fracture, plasma above and below the fracture zone would be set into motion. The essential point in this scenario was the postulate that, like fractures in the mechanical analogy, magnetic fractures once started would propagate into the adjacent, still stressed field of the overarching current circuit. The continuing supply of free magnetic energy would explain the longevity of individual active arcs way beyond the time scale of energy extraction between the source region in the outer magnetosphere and the AAR.

This model was cast into a set of simple physical relations supported by cartoons and was further developed in subsequent publications (Haerendel, 1988, 1994). The cartoon of Figure 4 of the latter study is reproduced here as Figure 1. It shows weakly oblique Alfvén waves attached to a region of U-shaped potentials, the "fracture zone," and extending upward to the generator plasma. On the bottom side, a region of multiply reflected waves is shown. The fracture zone has a leading edge propagating at very low speed compared with the Alfvén speed. Assumptions on the strength of a parametrized anomalous resistivity were shown to be consistent with observed auroral electron energies and energy fluxes. Much later Haerendel (2007) subjected this model to a thorough evaluation of energy storage and release in a current circuit with convective flow ultimately driven by a longitudinal pressure gradient. In the quasistationary picture, the transverse propagation was defined by the auroral arc width divided by a few Alfvénic time scales. Following (Lysak, 1981) the arc width was determined from the matching of the average Alfvénic wave impedance with the inverse of the total conductance according to (Lyons, 1980). A later publication (Haerendel, 2012) presented a refined definition of the arc width including the ionospheric contribution.

Most important for supporting the validity of the fracture model was the observational proof that auroral arcs are not frozen into the plasma frame but have a proper motion. This was achieved by simultaneous measurements of the electric field in the F region by means of an incoherent radar and optical tracing of the arc motion by Haerendel et al. (1993) and Frey et al. (1996). An in depth examination of the applicability of the fracture theory was performed by an ISSI team (Haerendel et al., 2012) by checking the consistency of data derived from all sky images of auroral arcs and from an overflight of the FAST spacecraft with predictions of the analytic theory (Haerendel, 2007, 2012). Six auroral arcs were seen to move into the interior of the large-scale current system at speeds as expected for the proper motions on the basis of arc width and Alfvénic time scale. The arcs appeared to emerge out of an Alfvénic arc at the border of the polar cap.

At this point it is opportune to refer to the notion of strong guide field reconnection (Chaston, 2015; Otto & Birk, 1993) as alternate explanation of the fracture process. Reconnection involves the transport of flux tubes laterally into the reconnection site. Thus there are relative motions between the plasma frames on *either* side of the reconnection site *before* stress release. Contrary to the high-beta reconnection, line-tying with the ionosphere must not be ignored. It is hard to conceive that such a situation can last for minutes. Furthermore, the stress release motions occur in opposite directions along the stress release site. This has strong implications on the spatial structuring of this site, that is on the interpretation of the rays or folds of the auroral arcs. In the reconnection scenario, the stress release motion can cover only the extent of a single ray. In the fracture process, it involves many consecutive rays, as we will see below. Most important is, however, the consequence that the converging inflows into the reconnection side forbid proper motions in one direction, in conflict with observations. In conclusion, high-guide field reconnection may exist for small-scale transient structures like the ones discussed by Chaston (2015), but not for the long lasting rayed evening arcs.

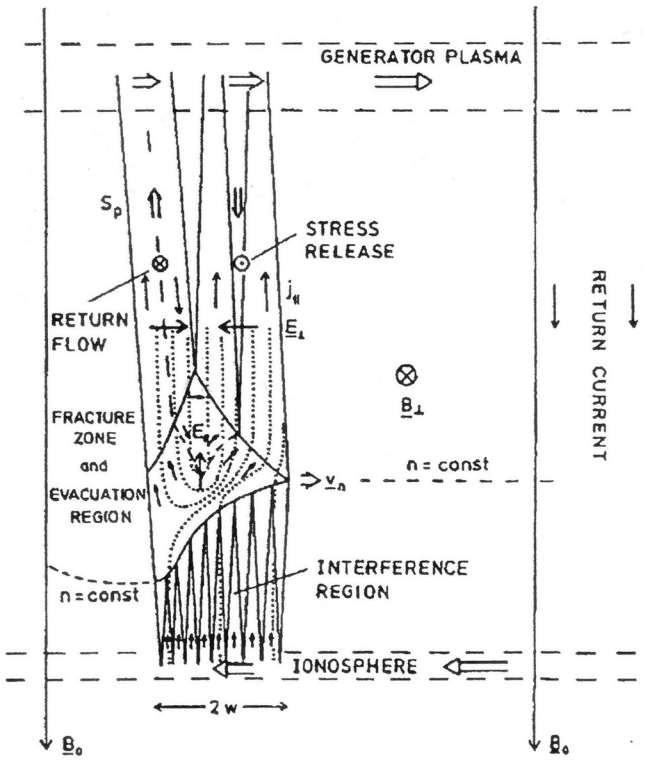

Figure 1. A model for the electromagnetic structure of the auroral current sheet in a straight-field-line geometry (Reprinted from Haerendel, 1994). Slightly oblique Alfvén waves attached to a slowly propagating "fracture zone" with speed, v_n, communicate the decoupling from the ionosphere by field-parallel potential drops to the generator plasma. On the leading edge (right) magnetic shear stresses are relieved and temporarily converted into plasma flows (inward pointing electric fields, $E_\perp$). The liberated magnetic energy is transported as Poynting flux, S_P, into the auroral acceleration region (fracture zone). Reverse flows (opposing electric field) on the trailing side restore to some extent the stress release. Dotted lines indicate electric equipotential contours. Upward ion acceleration leads to evacuation in the topside ionosphere. The "fracture zone" interacts with the ionosphere through small-scale damped Alfvén waves. The auroral current sheet in embedded in a large-scale current circuit between outer magnetosphere and ionosphere, corresponding to the evening side convection in the auroral oval.

On the basis of these observational checks one can regard the fracture theory as an adequate description of arcs embedded in the convection of the evening auroral oval, where weaker upward field-aligned currents extend over a few degrees of latitude, balanced by downward currents further equatorward thus constituting a wide energy reservoir. The analytical framework has proven to produce believable quantitative results. So, why do I want to revisit the fracture theory? The urge for that arose from comparing the cartoon shown in Figure 1 with my present understanding of its various elements. Its purpose is to visualize the physical structure of the acceleration region and the flows of energy and currents including the interaction with the ionosphere. As I will show below, this cartoon needs substantial revision in order to achieve consistency between optically observed arc structures and motions, on the one hand, and high-altitude electric field measurements, on the other hand. In Section 2 I will discuss the structure of the acceleration region with respect to height extent and energy storage, plasma flow, and transition to the ionosphere. A particularly intriguing subject is the interpretation of the U-shaped potential in the frame of the moving arc. This is the subject of Section 3 including the attached oblique Alfvén waves. Section 4 will finally present a new cartoon for the revised fracture model including a discussion of the currents and energy flows. In the Conclusions Section, all modifications will be summarized with respect to their physical meaning.

2. The Acceleration Region

2.1. The Height Extent of the Acceleration Region

In Figure 1 the acceleration region is shown as a distorted quadrangle with a sharp leading edge, from which the energy extraction out of the current circuit is initiated. It is postulated that the propagation of this edge is spontaneous, a consequence of the current dissipation just behind the front, alike to the propagation of a fracture in a solid body which is caused by the stress concentration at the leading edge. In the microphysical picture, molecular bonds are being broken in a solid body, in a magnetized plasma the decoupling electric fields are sustained by plasma turbulence. In his first study, Haerendel (1980) attributed this propagation to an anomalous diffusion process caused by ion-cyclotron turbulence. Later it appeared to be sufficient that dissipation behind the edge maintained steepening of the field-aligned current and thus sustained the forward propagation akin to an erosion process. The quasistationarity of the model allowed describing the proper motion of the arc in macroscopic terms (Equation 60 in Haerendel, 2007) as arc width over the energy dumping time:

$$v_n = \frac{w_{arc}}{4\tau_A} \quad (1)$$

The microphysics of the current dissipation and maintenance of the parallel electric field is hidden in the definition of w_{arc} (see above).

The sharpness of the leading edge in Figure 1 allowed to describe the wavefield as a bow wave of the propagating acceleration region. Furthermore, the energy influx along the wavefield was clearly separated from the region of energy conversion. This is, however, in conflict with the high incompressibility of the observed acceleration region and the very high value of the Alfvén speed, which renders the field as rather stiff and the electric field as practically electrostatic. According to Mozer and Hull (2001) the acceleration region extends between geocentric distances of r = 2.0 R_E and 3.5 R_E, that is, over about 10,000 km. Marioka

et al. (2010) distinguish between a low-altitude region below 5,000 km altitude and a high-altitude region between 6,000 and 12,000 km height. Even at the highest altitude of 3.5 R_E, the Alfvén speed ranges between 1.0 and 0.3 × 10^4 km/s for n = 1–10 cm^{-3}, respectively. This is much higher than the average Alfvén speed between acceleration region and generator (equator). This means that even in a cartoon it is not appropriate to attach the wave region to a sharp leading edge of the acceleration region at, say, 6,000 km height. Instead the leading edge of the acceleration region must be a blunt front of about 10,000 km extent.

There is another consequence. The acceleration region cannot be physically separated from the energy storage. In a current circuit driven by pressure gradients in the upper magnetosphere and closing through the ionosphere, a substantial fraction of the stored free magnetic energy resides in the height range of the to-become acceleration region. Equation 25 in Haerendel (2007) describes the height distribution (with the last but one term to be evaluated at ζ_{ion}). It varies solely as the function, $F_2(\zeta)$, plotted in Figures A2, with $\zeta = \sin\lambda$, where λ is the geomagnetic latitude. For instance, for a flux tube at L = 8 and a generator plasma beta of 3, the energy stored between r = 2.0 and 3.0 is 13.7% of the total. This means that the leading edge of the acceleration region, after initiation of parallel electric fields, will contain a substantial fraction of the initially converted energy before any inflow from above. This is important, because it may have an imprint on the visible appearance of the leading edge of the auroral arc. Keeping in mind this first revision of the cartoon in Figure 1, we can proceed to the next item.

2.2. Internal Structure of the Acceleration Region

Practically all sufficiently resolved electric field data obtained during transit of an inverted V event (e.g., Gurnett, 1972; Mc Fadden et al., 1999; Mozer & Hull, 2001) show that the field is very turbulent. Only the averaged field can conform to the theoretical U-shaped potential. Thus in a revisited model of the acceleration region, we have to rethink its internal structure. The observed turbulence applies to the perpendicular component of the electric field or the transverse plasma motions. The near-electrostatic nature of the electric field and the stiffness of the magnetic field imply that the transverse motions are shared by long rods of magnetic flux. However, they must not be regarded as completely rigid. They can be sheared and twisted. Even small amplitudes may contain large amounts of energy. A close theoretical equivalent is the numerical model of two-dimensional anisotropic MHD turbulence in an incompressible external magnetic field with high Reynolds numbers (e.g., Shebalin et al., 1983; Zhou et al., 2004), developed for the exploration of turbulence in fusion experiments like ZETA pinch and Tokamak. In our case the turbulence is enforced from outside by the sheared magnetic field and develops through the action of the resistive currents. So we should expect the appearance of turbulence cells and electric current sheets with cross-sections reminiscent of the 2 D simulation of Zhou et al. (2004). For illustration Figure 5 of that study is reproduced here as Figure 2. In the auroral situation, there is a preferred direction imposed on the anisotropy of the turbulence, namely the direction of stress release. This implies that the internal structure should consist of sheared long rods, embedded in a flow and quickly breaking into vortices. This leads us to the auroral rays.

Hallinan and Davis (1970) observed auroral rays along the magnetic field lines where they appear as moving folds or curls. They attributed the origin to a sheet-beam instability and the motions to an E × B drift of the plasma. When observed across an arc, the motions were invariably found to be oppositely directed. Haerendel et al. (1996) also observed moving auroral rays in the magnetic zenith by low light level TV. In addition, the ionospheric electric field was determined with the EISCAT UHF radar. Viewed along the magnetic field lines, the rays appeared as moving folds at the leading edge of the arc. In the rear, fainter counterflows appeared. Naturally this was attributed to the existence of a U-shaped potential and converging electric fields on either side of the AAR. However, the moving structures were asymmetric in brightness and speed, strongly favoring the arc's leading edge. For this reason, auroral rays most often appear as moving in one direction only when observed from the side. Thanks to the radar measurement of the electric field, the background plasma frame could be determined. Its motion was at least one order of magnitude slower than the folds along the arc. This was a confirmation that the electric fields at high altitudes are shorted out by the potential drops through the acceleration region. Furthermore, a slow proper motion of the arc could be assessed. This means that one could identify leading and trailing edges of the arc. Converting the flow speeds into converging electric fields and multiplying with the transverse scales produced potential drops consistent with the optical properties of the arc.

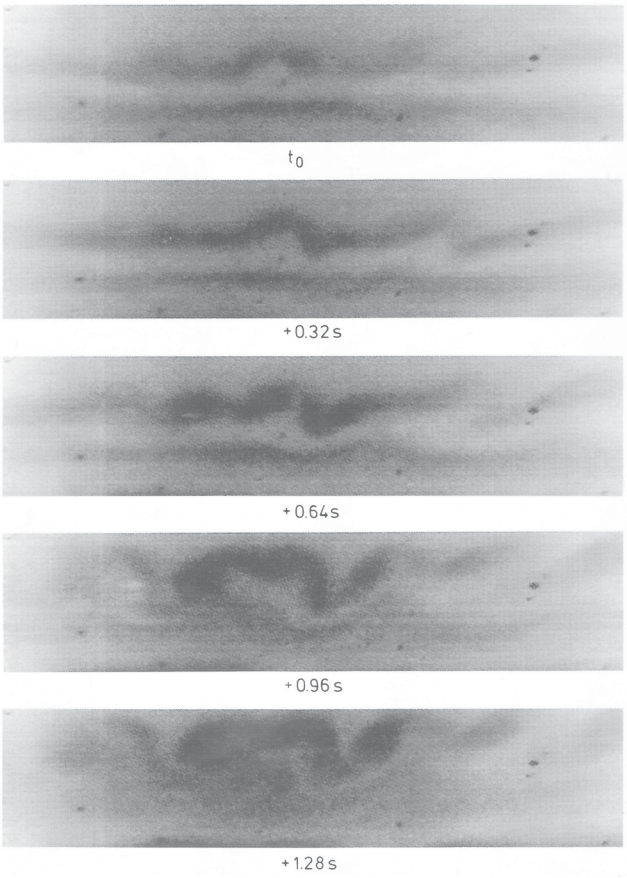

Figure 2. Development of folds at the leading edge of an auroral arc into curls (reprinted from Haerendel et al., 1996). View antiparallel to B with south at the top.

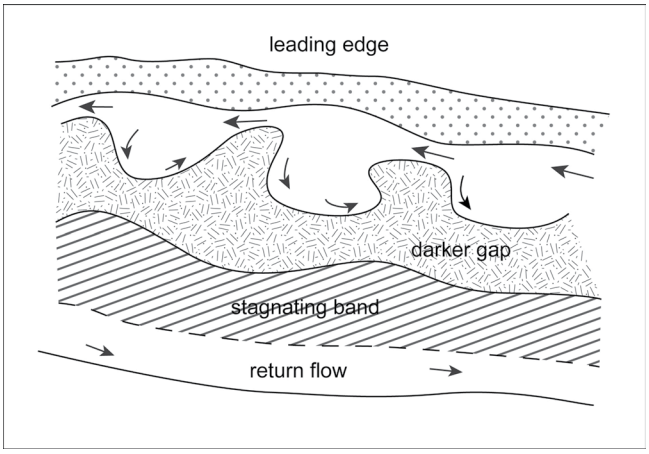

Figure 3. Cartoon showing the stress release flow at the arc's leading edge breaking partially into formation of anticlockwise curls.

The authors attributed the formation of folds, curls, and rays to a Kelvin-Helmholtz instability of the stress release flow at the leading edge of the propagating arc. They also noted the tendency of the folds to develop into curls in the counterclockwise sense, as already discovered by Hallinan and Davis (1970). This is documented in Figure 3, a reproduction of Figure 3 of Haerendel et al. (1996). The Video S2, provided as supporting information (https://projects.mpe.mpg.de/space-plasma/polarlight.html), displays more convincingly that it is only a fraction of the westward flow contour that breaks off into the reverse direction. This can be noticed with practically all folds at the leading edge. It is remarkable that the beginning flow reversal exhibits the highest brightness. It suggests that it is here where the energy conversion maximizes. However, part of the westward flow on the leading edge continues at reduced thickness and brightness. In the light of the above quoted resemblance with a 2-D MHD turbulence, it can be interpreted as a convection cell breaking partially into a reversed and a continuing flow during each wave period. A typical observation with a bit of interpretation is sketched in Figure 4. Similar, but less pronounced developments one can observe deeper in the luminosity band of the arc.

We are hitting here an essential point. Breaking of the turbulence cells means that the plasma motion, which is a consequence of magnetic stress release or fracture, continues unimpeded only for onefold period. The energy contained therein is quickly breaking into smaller scales and subsequently into random directions, as suggested by the lack of structure further into the arc. Why is that so? The main reason is probably that the incompressibility of the main field does not allow unimpeded directional flows and thus enforces partial reversals and absorption of the momentum by the main field on time scales short compared with τ_{arc}, the time scale of complete stress release. With this insight we can resolve the conflict between the two estimates for the stress release amplitudes in Equations 81 and 84 of (Haerendel, 2007) of 62 km and 1,204 km, respectively. The first applies to the displacement of the foot of a field line between front and rear of the auroral current sheet, due to the changing inclination. The latter number was derived from a displacement by the stress release flow during one-half of τ_{arc}. In order to solve this conflict, the author assumed that like in the analogy with a breaking rod there was an overshoot of the motion of the disconnected parts. This is what would occur when the breaking body is embedded in air or vacuum. However, the moving magnetized plasma structures fragment into turbulent structures and deposit momentum and energy in multiple steps in the magnetic field at time scales much shorter than τ_{arc}. However, the question remains: Does this prevent completely any overshoot? If there is none, what causes the return flow on the trailing edge of the arc? We will address these intriguing questions in Section 3.

In any case, we can conclude from the above that the optically observable internal motions of an arc are consistent with the turbulent electric fields measured from spacecraft in and above the acceleration region. The development of folds shows that the turbulence is initiated by a shear flow instability of the stress release motions at the arc's leading edge. The further evolution of the turbulence is hidden in diffuse brightness distributions. Electric field measurements with the S3-3 spacecraft (Mozer et al., 1977) crossing an arc at a height of 7,600 km revealed temporal changes of the electric field with frequencies below 200 Hz. Attributed to

the electrostatic ion-cyclotron waves, this corresponds to spatial scales of about 120 m. On the other hand, there are also electric field pulses consistent with the initial fold and curl structures. McFadden et al. (1990) observed dispersive bursts of field-aligned electrons and suggested a connection with the visible rays of the arc. This is supported by the brightness concentration in the beginning curl structure.

Inspired by the quoted simulations of 2-D MHD turbulence, one may visualize the internal structure of the acceleration region as consisting of moving field-aligned current concentrations and rotations of short duration. The turbulence is not homogeneous. It is a mix large-scale eddies, the observed curls, and microscopic electrostatic turbulence. If one tries to estimate related transverse diffusion coefficients, one obtains values ranging between (0.3–3.0) $\times 10^7$ m^2/s, the lower value based on the quoted satellite data (Mozer et al., 1977), the higher one based on curl sizes of typically 5 km and turnover times of 1 s, as exhibited in Figures 2 and 3. If one would settle on the geometric mean and typical transit times of an arc of 150 s (Haerendel, 2007), one would obtain arc widths of about 35 km. In spite of the crudity of such an estimate, it confirms that turbulent energy conversion is consistent with the typically observed widths and proper motions of structured arcs embedded in the evening convection of the auroral oval.

2.3. Transition to the Ionosphere

The interference region appearing in the cartoon of Figure 1 underneath the acceleration region, was introduced by the author (Haerendel, 1988) in order to cope with the short Alfvénic propagation times vis-à-vis the slow transverse proper motion of the arc. In spite of the high reflectivity of the lower ionosphere the waves may be strongly damped because of their narrow transverse scales (cf. Haerendel & Mende, 2012). Such waves may exist, but of more importance are rather abrupt transitions between the low-density auroral cavity and the denser topside ionosphere. McFadden et al. (1999) reported measurements with the FAST mission suggesting the existence of narrow potential fingers within an inverted V situation reaching down toward the denser ionosphere. They are recognized by the presence or absence of upward ion beams and absence or presence of dense ionospheric plasma, respectively. From measurements with the Polar mission, Mozer and Hull (2001) found the lower border of the AAR between 1.0 and 1.5 R_E to be corrugated by potential fingers.

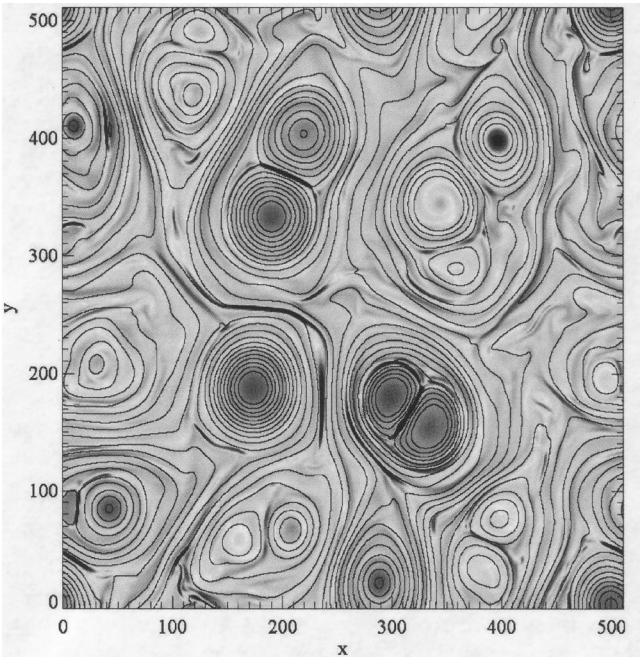

Figure 4. Magnetic field lines from a spectral-method simulation of 2D MHD turbulence and associated randomly occurring electric currents (Reprinted from Zhou et al., 2004). Gray shading shows magnitudes of the currents with most intense currents out of the plane in white and into the plane in black.

Direct observations of localized, large-amplitude parallel electric fields in upward current regions have been made by Mozer and Kletzing (1998), Ergun et al. (2002), Hull et al. (2003), and Ergun et al. (2004). Such fields were mostly found at the boundary of auroral cavities and estimated to contain between 10% and 50 % of the total auroral potential (Mozer & Hull, 2001). Ergun et al. (2000) addressed these findings theoretically first by using Vlasov-Poisson equations in a 1-D geometry with prescribed overall potential drop. They found two sudden transitions with appreciable potential drops, one near Earth due to changes in the electron components and a higher one characterized by sudden changes in the ratio of cold and hot ions. Somewhat later, Ergun et al. (2002) addressed the same problem in a planar geometry of stationary, oblique double layers with widths of about 10 km. It is not obvious how such oblique double layers match with the potential fingers and their horizontal geometry appearing in the cartoons. However, they offer a convincing scenario for the auroral evacuation process as proposed by Haerendel (1999). In any case we can conclude that the lower boundary of the acceleration region is corrugated by multiple narrow regions of concentrated potential drops terminated by sudden transitions to colder and denser plasma. They contribute substantially to the overall acceleration of both electrons and ions. Figure 5, taken from Figure 5 of Mozer and Kletzing (1998), serves as a representative cartoon.

3. Propagating U-Shaped Potentials

Earlier theoretical models of electrostatic U-shaped potentials were based on ion dynamics (Swift, 1975, 1979) or ion anisotropy (Chiu & Cornwall, 1980) and were completely static. MHD models were employing anomalous resistivity and were typically nonstationary involving multiple reflections from ionosphere and generator plasma (Lysak & Dum, 1983). The U-shape is essentially owed to the electrostatic boundary conditions and the width of the considered current sheet. It was the long lifetime of structured auroral arcs embedded in the auroral convection on the evening side what led the author to abandon static or nonstationary models and introduce quasistationary, slowly propagating U-shaped potentials with oblique Alfvén wings attached (Haerendel, 1980, 1988, 1994). The latter are progressively unshearing the magnetic field and channel the liberated magnetic energy into the acceleration region. This scenario throws a completely new light on the U-shaped potential. It now has a temporal dimension, a leading and a trailing side, and is thus completely asymmetric. This applies also to the converging electric fields. At the front side magnetic energy is liberated by a stress release process following the propagating oblique Alfvén fronts. The transverse electric field expresses the stress release motion, which temporarily contains the liberated energy in form of kinetic energy of flow. Since this energy is continuously emptied into the acceleration region, the transverse electric field thus expresses also the downward Poynting flux into the AAR. While this physically consistent scenario has proven to provide also quantitative checks (e.g., Haerendel, 2007; Haerendel et al., 2012), a proper interpretation of the opposing electric field on the trailing side is not a simple matter. It represents plasma motions opposite to those connected with the stress release and is thus restoring, at least partially, the original shear stresses. In the framework of the magnetic fracture model, the question arises what is driving this return motion.

Before we turn to this question, we must remember that in the new interpretation the U-shaped potential has two intimately connected aspects. First, as discussed in Section 2.2, it is strongly disturbed by the existence of a nearly two-dimensional turbulence. This means that any equipotential contours drawn through the acceleration region are meant to represent averages of a turbulent field with much higher peak values of the electric field. Second, there is no longer a strict temporal sequence of the energy liberation and conversion processes across the arc. It is broken by an instantaneous transport of energy and momentum perpendicular to the magnetic field and thus destroys a simple temporal labeling of sequential longitudinal cuts through the arc.

Returning now to the overarching temporal sequence, we look again carefully at the observations presented in Haerendel et al. (1996) and at the Video S2 added as supporting material (https://projects.mpe.mpg.de/space-plasma/polarlight.html). The video as well as the brightness scan shown in their Figure 5 exhibit a clear asymmetry in energy flux as well as in the flow pattern. The leading westward directed stress release flow dominates the brightness distribution. It is followed by a brightness minimum and a seemingly stagnating flow. In the rear, a diffuse return flow is clearly discernible at much reduced brightness. The preponderance of a westward flow in the downward energy flux and the much narrower region of reverse flow with low energy flux suggest that there is a substantial S-shape contribution to the average potential distribution. However, this is only part of the reason for the asymmetry.

The propagation time of the arc by its width contains a few (or several) Alfvén travel times to the generator or back. Hence there must be a feedback. What happens was quantitatively analyzed by Haerendel (2007). The generator of the auroral current sheet is a current generator (Lysak, 1990). When the stress release front, initiated at the AAR, has arrived at the hot generator plasma, it is reflected and the transverse electric field does not change sign. However, the reflection process takes time and the source plasma is strongly affected. First, the stress balance between the driving pressure force and the magnetic shear stresses is disturbed and leads to a plasma acceleration in the direction of the pressure force. After about two single-path travel times of an Alfvén wave is the plasma fully set into motion and in effect tries to restore the perturbation field. However, as the wave travels downward, it meets with another restoring wave coming from below. By moving the plasma in the reverse direction, it also acts in the sense of restoring the perturbation field. The interaction of the two waves may be the origin of the stagnation region in the central arc (Figure 3).

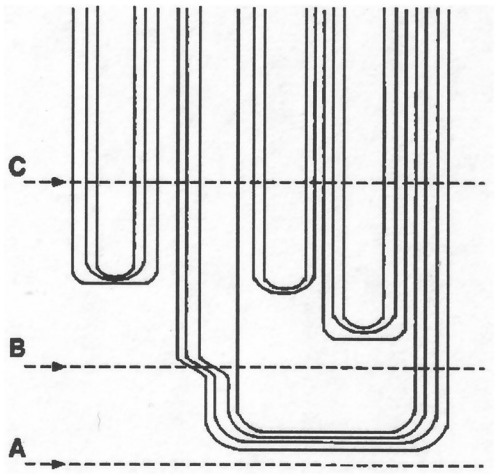

Figure 5. Equipotential of a quasistatic electric field in a uniform magnetic field, illustrating the presence of finger-like structures with large parallel electric fields at the transition to the denser ionosphere (Reprinted from Mozer & Kletzing, 1998).

What is the nature of the restoring force from below? It is related to the tricky question about the driver of the reverse flow. The near-electrostatic nature of the potential distribution in an incompressible magnetic field should lead to a U-shaped potential also in a propagating current sheet. A dynamic interpretation of what happens may be the following. The decoupling of the field from the ionosphere must also allow magnetic flux transport across the arc, for instance an interchange motion between the front section and the rear. In the front, there is this antagonism between the drag from above by the stress release flow and the resistance against magnetic flux pile-up. As discussed above, that leads to local counter-clockwise rotations and return flows (see Figure 4). The ensemble of these eddies with reverse motions must naturally constitute a source of reverse momentum which is transported toward the rear section as the arc propagates. Where the cross-field mobility of the turbulence comes to a stop, a systematic reverse flow must arise.

A completely different interpretation was presented by Haerendel (2007). He proposed an overshoot of the stress release motion and a subsequent return flow (see his Figures 8 and 9). When calculating the stress release motion over one-half of the total arc time, he found a displacement of the low-altitude plasma much larger than expected from the net reduction of the transverse field component behind the auroral current sheet. This estimate was based on the assumption of an unimpeded stress release flow. However, as we saw in Section 2.2, the flow brakes quickly into turbulent cells. Furthermore, what could constitute the restoring force? It can't be the elastic force of the whole flux tube, since, as we saw above, the field is not firmly anchored in the generator plasma. Quite to the contrary, the response from above drives the plasma in the initial stress release instead of the reverse direction. The idea of a large overshoot must be abandoned.

We encounter a strange situation. As confirmed by many measurements of the magnetic perturbation field, also the rear section of an arc (acceleration region) is pervaded by upward field-aligned currents. As the arc propagates, the shear field in the plasma frame is being reduced and should drive the plasma in the same sense of stress release. On the other hand, a reversed mean electric field is consistent with the presence of a reverse flow, which would lead to an enhancement of the shear field. This is a real enigma. It means that, while in the front section the inward pointing electric field is owed to the transport of momentum from the stress release, the reverse flow and opposing electric field in the rear are not owed to a release of shear stresses, but to the incompressibility of the main magnetic field. The action of the latter overturns the action of any still existing stress release in the height range of the acceleration region. This superposition of two antagonistic forces is only possible because the magnetic field is not frozen in the plasma due to the presence of anomalous resistivity and decoupling from the ionosphere. However, above this region, in the wavefield, the magnetic field is frozen-in. Does it respond to shear stresses applied from below thus bringing the perturbation field a bit back into the upstream direction? This would be the feedback from below connected with an upward directed Poynting flux supplying the energy needed for the partial restoration of the perturbation field. However, in this case the upward field-aligned currents must be diverted toward the arc's center. I will return to these implications in the next section.

An upward Poynting flux in the rear was already proposed by Haerendel (1994, 2007) (see Figure 1), who connected it with a hypothetical overshoot. However, this was an internally conflicting suggestion, since in case of an overshoot as restoring force, the Poynting flux should have come from above. The here offered revised origin of the return flow lies in the transport of reverse momentum through the auroral current sheet due the incompressibility of the magnetic field in the acceleration region. Thus the Poynting flux must come from below. According to the supplied video the discernable return flow fills only a small section in the rear of the arc, whereas much of the reversed electric field is found in a turbulent stagnation region, where feedback from above and below oppose each other.

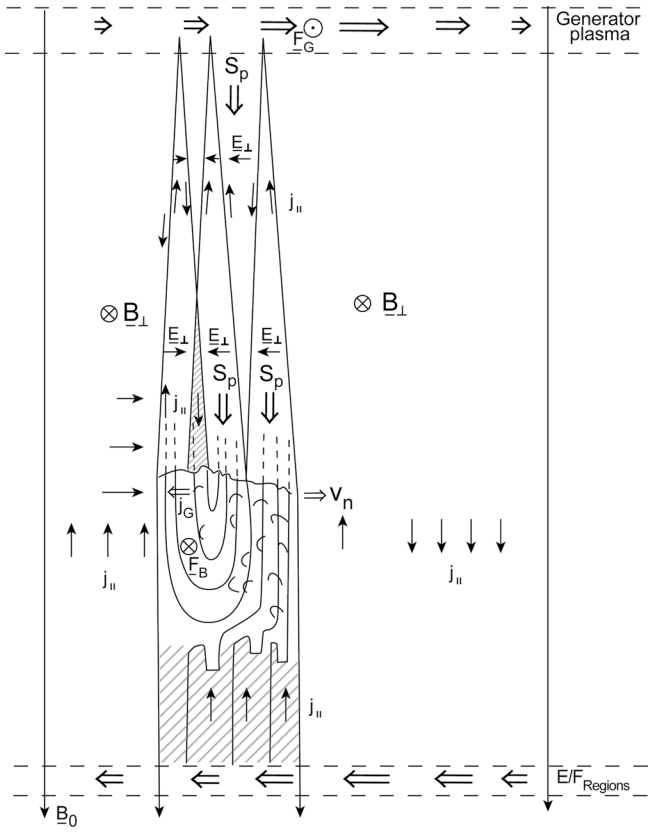

Figure 6. Revised fracture model. Slightly oblique Alfvén wave fronts attached to the auroral acceleration region or "fracture zone" in a straight field lines geometry. The upward auroral current sheet is embedded in a large current circuit between generator region (outer magnetosphere) and the E and F regions of the ionosphere. The auroral acceleration region is structures by a mean U-shaped potential with potential fingers toward the ionosphere and a substructure of nearly 2-D magnetic turbulence. The wavefield contains downward Poynting flux from the magnetic stress release in the front part, feedback from the generator in the center, and a stress restoring wave with balanced currents and upward Poynting flux in the rear, driven from the reverse flow in the acceleration region. Note a downward current adjacent to the rear wave.

4. A Revision of the Magnetic Fracture Model

In Sections 2 and 3 I have discussed four aspects of the fracture model, the height extent of the acceleration region, its internal structure, its lower border versus the cool, dense ionosphere, and the temporal-spatial nature of the average, nearly electrostatic potential. This must naturally lead to a revision of the cartoon found in (Haerendel, 1988, 1994, 2007). It is not an easy task. One can only display the average sequence of events between the leading edge and the rear and, as far as the currents are concerned, the embeddedness in a large circuit between outer magnetosphere and ionosphere. What is rather difficult to represent graphically, is the role of the nearly 2-D turbulence. From the coupling between longitudinal flows and shear stresses, on the one hand, and normal magnetic forces, on the other hand, it transpires that there must be perpendicular currents which, integrated over the height range, divert upward currents inside the turbulent region. Where and how this happens, is hard to assess. Therefore, the new view, condensed into the cartoon of Figure 6, will not be definite about the current distribution inside this region. This is a subject for further work.

In comparison with the cartoon of Figure 1, the following changes have been applied to that of Figure 6. First, the height extent of the acceleration region is substantially increased and has a blunt leading edge (see Section 2.1). It remains open, whether it is a strict equipotential surface or corrugated by small-scale turbulence, which may be more realistic. Second, the internal potential structure (see Section 2.2) is represented as before by average equipotential lines. However, now they exhibit also an S-shape contribution extending to the lower ionosphere. On the upper end of the acceleration region, one cannot continue the equipotential lines, since here the induction field clearly dominates. The important 2-D turbulence is only represented by graphic signs for counter-clockwise internal flows. Third, the bottom of the acceleration region (see Section 2.3) contains a few indications of downward extending potential fingers housing strong local parallel electric fields. As in Figure 1, the cartoon uses straight magnetic field lines and represents a rather extended equatorial source region as a thin generator layer. The wavefield, consisting of weakly oblique Alfvén waves, is represented by wave fronts and current arrows ($j_\parallel$). The average transverse electric field direction is designated by thin arrows ($\underline{E}_\perp$) and the Poynting flux ($\underline{S}_p$) as broad open arrows. At variance from Figure 1, feedback from the generator region is shown to interfere with the feedback from below. The existence of such an interference region is a conjecture. Its observational signature will be strongly fluctuating small-scale electric fields. At two of the wave fronts, downward currents are indicated, one belonging to the feedback from above, the other to the feedback from below.

The wavefield emerging from the feedback from below deserves special attention. It receives momentum and energy from the reversed flow enforced in the acceleration region. A local generator force, $\underline{F}_B$, of the currents associated with the wavefield and the respective generator current, $\underline{j}_G$, are shown. The wavefield is characterized by two wave fronts with upward and downward currents, respectively, meeting at the source region. This represents the fact that the upward directed Poynting flux has a negative divergence delivering only the energy needed to restore a fraction of the original shear field. This fraction may correspond, at least in part, to the additional energy inflow by the feedback from above. What is deliberately not shown, is the continuation of the field-aligned currents flowing up from the lower ionosphere. As discussed above, they become diverted into perpendicular currents throughout the whole acceleration region. But where and how remains somewhat obscure at this point.

As in Figure 1, the auroral current sheet is embedded in a global current circuit of Boström's (1964) Type 2 and propagates equatorward with speed, v_n. The currents in ionosphere and source region are shown by open arrows. The connecting currents, downward currents at low latitude and upward currents at high latitude, are labeled by thin vertical arrows. In total, this represents the global circuit set up by the sunward convection in the evening auroral oval during and after a substorm. Its poleward section contains the energy reservoir from which the equatorward propagating arcs are being fed by reducing the increasing perturbation field. A good manifestation of this situation is presented in Figure 10 of Haerendel et al. (2012).

A certain subtlety can be found in the contour of the perturbation field of that Figure 10. Behind some of the arcs, a short change of the slope indicates a downward current in the rear of the upward current sheet. Although the accuracy of the magnetic field measurement is not very high, this is a valid feature which surprisingly agrees with the existence of the trailing wavefield. With its balanced currents, this wavefield just changes progressively the inclination of the magnetic field a bit toward the original shear field. This means that behind the arc the shear field is somewhat less reduced than what would correspond to the auroral sheet current. Therefore, there must be an additional downward current correcting for that. In other words, not all the magnetic energy contained in the shear field through the arc is converted. A fraction is being restored owing to the discussed action of the magnetic field compression. Unfortunately, there is little literature on embedded arcs from medium altitude spacecraft with sufficient temporal resolution. Two events in the published literature showing the downward current may be found in Figure 2 of Lotko et al. (1998) and in Figure 2 of Lynch et al. (2015).

By contrast to the substantial changes of the cartoon for the auroral current sheet with respect to the former one, the formalism describing quantitatively energy source, storage, release, and conversion, as laid down extensively in (Haerendel, 2007), remains unaffected by the new interpretations presented here. There are just two exceptions. Equations 84 and 85, which estimate the overshoot, have no basis any more. The electric field expression in Equation 83 does not correspond to the whole decoupling or stress release motion but can only apply to the peak flows observable in the video as supporting material. The cartoons in Figures 8 and 9 of that study will have to be revised.

5. Conclusions

Far extending structured auroral arcs appearing in the evening auroral oval during and after substorms belong to the most striking auroral phenomena, in particular because of their longevity. This is in clear contrast to arcs in the late night auroral convection, where such arcs can appear inside downward current regions as isolated events (McFadden et al., 1990). They are probably owed to episodic narrow enhanced flow regions. The embedded evening arcs lend themselves to theory and quantitative comparison, because no special event needs to be invoked for their appearance. They derive their energy simply from an extended energy reservoir in terms of a Type 2 current system after Boström (1964). This is proven by the existence of proper motions with respect to the local plasma (Frey et al., 1996; Haerendel et al., 1993, 2012), which are in quantitative agreement with the progressive extraction of the free magnetic energy. Calling this process *magnetic fractures* had two reasons, the release of magnetic, hence elastic energy and the spontaneous propagation of the fracture zone. These are basic phenomena of any fracture theory. The author has developed this scenario between 1980 and 2007 and has illustrated it by the cartoon in Figure 1. Since cartoons are meant to be helpful in conveying essential physical concepts, it is an obligation to revise them when new insights have been gained into the actual physical process. This is the objective of this study and condensed into the revised cartoon in Figure 6.

There are four modifications, while the overall concept, the embeddedness of the auroral current sheet in a large current circuit, remains unchanged. The first modification (Section 2.1) pertains to the height extension of the acceleration region of the order of 10,000 km. However, there is more to it. It is emphasized that this height range also contributes substantially to the energy stored by the shear field. The finding that in most cases auroral rays are only present in the leading section of the arc suggests that the stress release within this height range with its nearly incompressible field contributes strongly to their formation.

This leads directly to the second modification (Section 2.2) which brings the model into agreement with the generally observed large-amplitude fluctuations of the converging electric fields in the acceleration region. It is argued that these fluctuations are a manifestation of a nearly 2-D turbulence owed of the incompressibility of the magnetic field. An auroral movie, added as supporting information, gives deep insights into the breaking of the auroral folds into curls and, no longer optically resolvable, into smaller turbulent elements. This is a consequence of the stress release flow being strongly impeded by the incompressibility of the magnetic field.

The third modification (Section 2.3) does away with the conjecture of the earlier studies that the transition to the ionosphere can be described by a zone of interfering Alfvén waves. Instead the existence of *potential fingers* is incorporated, since there is ample evidence from data and theory that such regions with sudden changes of density and strong potential drops, described as electrostatic double layers, are quite common. This has a strong impact on the height distribution of the total potential drop, but is of little consequence for the arc model.

The fourth modification (Section 3) deals with the average potential distribution within the acceleration region, the attached wave fields, and the associated currents. It is actually the heart of this study and presents some novel concepts. In its center stands the interpretation of the U-shaped potential, structuring the acceleration region, in a propagating current sheet. It requires replacing a simple electrostatic interpretation by a dynamic one. Whereas in the front section of the arc the average electric field is the expression of stress release motions, the understanding of the reversed field in the trailing section is not obvious. For the wavefield above the acceleration region, where frozen-in conditions prevail, it means that there is a reversed flow, restoring somewhat the released magnetic perturbation field. However, this is difficult to reconcile with the existence of upward directed currents also in the rear section.

In order to cope with this apparent inconsistency, with which the author struggled for a long time, one must give up the strictly temporal interpretation in the plasma frame. As already discussed in Section 2, small-scale reverse flows behind the leading stress release flow lead to transport of momentum and magnetic flux in the normal direction through the arc. This is owed to the incompressibility of the magnetic field which forbids magnetic flux pileup. Therefore, drag in the stress release direction in the front section must to a large extent be balanced by a reversed flow in the rear. This action, due to magnetic normal stresses, obviously dominates any residual stress release.

Little is known about the wavefield above narrow embedded arcs in the evening oval. One should expect that the wavefield above the rear section experiences a drag from below in the reverse direction. This means that the plasma in the acceleration region underneath constitutes a voltage generator. The related current system must be balanced. However, since the result is a change of the inclination of the field lines, Ampere's law requires the presence of a downward current. And indeed, a few cases have been cited above which testify for the existence of such a current (see Section 4). This is indicated in the cartoon of Figure 6. However, the here presented solution for the wavefield in the rear implies that the upward field-aligned currents cannot continue into the wavefield. In the rear of the acceleration region they must be diverted toward the interior and continue upward into the generator region. The total stress release by the passage of the upward current is mitigated by the reverse flow in the rear section. The downward current is the witness.

Spontaneous propagation of structured auroral arcs in the evening auroral oval has been proven beyond doubt by observations. In spite of its simplicity, the concept of their origin by the release of magnetic shear stresses has proven to be not so easily cast into a convincing theoretical scenario. The difficulties for a proper interpretation reside, on the one hand, in the lack of sufficiently resolved observations in and above the acceleration region and, on the other hand, in the fact that the arc's current sheet is only an element in a not really understood global current system. While the concept of magnetic fractures may aid the intuition, one encounters conceptual problems with the incompressibility of the magnetic field inside the fracture zone. This study tries to present a consistent interpretation.

In closing, I want to point out how little theoretical work has been done on integral auroral arc systems, in contrast with the extensive work done on the involved local plasma processes. The reason is, of course, that the physics is greatly changing along an auroral current sheet between equator and ionosphere. This poses particularly great challenges on any numerical modeling effort. The practical impossibility of observing

simultaneously the total involved system also works in a discouraging sense. All the same, this should not deter from, but rather encourage coordinated satellite missions continuing and going beyond the great achievements of missions like Viking, Freja, FAST, and Polar.

Data Availability Statement

A video of an auroral arc is added as supporting information with the permission of the Max Planck Institute for extraterrestrial Physics, Garching/Germany (https://projects.mpe.mpg.de/space-plasma/polarlight.html). The low-light-level TV camera system was operated by the late Werner Lieb.

Acknowledgments
I enjoyed discussions with Dr. R. E. Ergun, in particular on the effect of magnetic incompressibility on the stress release motions.

References

Ackerson, K. L., & Franck, L. A. (1972). Correlated satellite measurements of low-energy electron precipitation and ground-based observations of a visible auroral arc. *Journal of Geophysical Research*, *77*, 1128.
Block, L. P. (1972). Potential double layers in the ionosphere. *Cosmic Electrodynamics*, *3*, 349.
Boström, R. (1964). A model of the auroral electrojets. *Journal of Geophysical Research*, *69*, 4983–4999.
Chaston, C. C. (2015). Magnetic reconnection in the auroral acceleration region. *Geophysical Research Letters*, *42*, 1646–1653. https://doi.org/10.1002/2015GL063164
Chiu, Y. T., & Cornwall, J. M. (1980). Electrostatic model of a quiet auroral arc. *Journal of Geophysical Research*, *85*(A2), 543–556.
Ergun, R. E., Andersson, L., Main, D., Su, Y.-J., Newman, D. L., Goldman, M. V., et al. (2004). Auroral particle acceleration by strong double layers: The upward current region. *Journal of Geophysical Research*, *109*, A12220. https://doi.org/10.1029/2004JA010545
Ergun, R. E., Andersson, L., Main, D., Su, Y.-J., Newman, D. L., Goldman, M. V., et al. (2002). Parallel electric fields in the upward current region of the aurora: Numerical solutions. *Physics of Plasmas*, *9*(9), 3695–3704.
Ergun, R. E., Carlson, C. W., McFadden, J. P., Mozer, F. S., & Strangeway, R. J. (2000). Parallel electric fields in discrete arcs. *Geophysical Research Letters*, *27*(24), 4053–4056.
Evans, D. S. (1968). The observations of a near monoenergetic flux of auroral electrons. *Journal of Geophysical Research*, *73*, 2315
Franck, L. A., & Gurnett, D. A. (1971). Distributions of plasmas and electric fields over the auroral zones andpolar caps. *Journal of Geophysical Research*, *76*, 6829
Frey, H. U., Haerendel, G., Knudsen, D., Buchert, S., & Bauer, O. H. (1996). Optical and radar observations of the motion of auroral arcs. *Journal of Atmospheric and Terrestrial Physics*, *58*, 57–69.
Fridman, M., & Lemaire, J. (1980). Relationship between auroral electron fluxes and field aligned electric potential difference. *Journal of Geophysical Research*, *85*, 664–670.
Goertz, C. K. (1981). Discrete breakup arcs and kinetic Alfven waves. In S.-I., Akasofu & J. R., Kan (Eds.), *Physics of auroral arc formation, geophysical monograph series 25* (pp. 451–455). Washington, DC: American Geophysical Union.
Gurnett, D. A. (1972), Electric field and plasma observations in the magnetosphere. In E. R. Dyer (Ed.). *Critical problems of magnetospheric physics* (pp. 123–136). Washington, DC: National Academy of Sciences.
Haerendel, G., Rieger, E., Valenzuela, A., Föppl, H., & Stenbaek-Nielsen, H. (1976). *First observation of electrostatic acceleration of barium ions into the magnetosphere*, Proceedings of the Symposium on Present and Future European Sounding Rocket and Balloon Research in the Auroral Zone. (203–211). Paris, France: European Space Agency.
Haerendel, G. (1980). Auroral particle acceleration - An example of a universal plasma process. *ESA Journal*, *4*, 197–210.
Haerendel, G. (1988). Cosmic linear accelerators. In T. D. Guyenne & J. J. Hunt (Eds.), *Proeedings of joint Varenna-Abastumani school & workshop on plasma astrophysics, ESA SP-285* (Vol. 1, pp. 37–44). Paris, France: European Space Agency.
Haerendel, G. (1994). Acceleration from field-aligned potential drops. *The Astrophysical Journal - Supplement Series*, *90*, 765–774.
Haerendel, G. (1999). Origin and dynamics of thin auroral arcs. *Advances in Space Research*, *23*(10), 1637–1645.
Haerendel, G. (2007). Auroral arcs as sites of magnetic stress release. *Journal of Geophysical Research*, *112*, A09214. https://doi.org/10.1029/2007JA012378
Haerendel, G., Buchert, S., LaHoz, C., Raaf, R., & Rieger, E. (1993). On the proper motion of auroral arcs. *Journal of Geophysical Research*, *98*, 6087–6099.
Haerendel, G., Frey, H. U., Chaston, C. C., Amm, O., Juusola, L., Nakamura, R., et al. (2012). Birth and life of auroral arcs embedded in the evening auroral oval convection: A critical comparison with theory. *Journal of Geophysical Research*, *117*, A12220. https://doi.org/10.1029/2012JA018128
Haerendel, G., & Mende, S. B. (2012). Magnetosphere-ionosphere coupling and scale breaking of a plasma cloud in the magnetosphere. *Journal of Geophysical Research*, *117*, A09233. https://doi.org/10.1029/2012JA018021
Haerendel, G., Olipitz, B. U., Buchert, S., Bauer, O. H., Rieger, E., & LaHoz, C. (1996). Optical and radar observations of auroral arcs with emphasis on small-scale structures. *Journal of Atmospheric and Terrestrial Physics*, *58*, 71–83.
Hallinan, T. J., & Davis, T. N. (1970). Small-scale auroral arc distortions. *Planetary and Space Science*, *18*, 1735–1744.
Hull, A. J., Bonnell, J. W., Mozer, F. S., & Scudder, J. D. (2003). A statistical study of large-amplitude parallel electric fields in the upward current region of the auroral acceleration region. *Journal of Geophysical Research*, *108*(A1). https://doi.org/10.1029/2001JA007540
Kindel, J. M., & Kennell, C. F. (1971). Topside current instabilities. *Journal of Geophysical Research*, *76*, 3055–3078.
Kintner, P. M., Kelley, M. C., & Mozer, F. S. (1978). Electrostatic hydrogen cyclotron waves near one Earth radius altitude in the polar magnetosphere. *Geophysical Research Letters*, *5*, 139
Knight, S. (1973). Parallel electric fields. *Planetary and Space Science*, *21*, 741–750.
Lotko, W., Streltsov, A. V., & Carlson, C. W. (1998). Discrete auroral arc, electrostatic shock and suprathermal electrons powered by dispersive, anomalously resistive field line resonance. *Geophysical Research Letters*, *25*(24), 4449–4452.
Lynch, K. A., Hampton, D. L., Zettergren, M., Bekkeng, T. A., Conde, M., Fernandes, P. A., et al. (2015). MICA sounding rocket observations of conductivity-gradient-generated auroral ionospheric responses: Small-scale structure with large-scale drivers. *Journal of Geophysical Research: Space Physics*, *120*, 9661–9682. https://doi.org/10.1002/2014JA020860

Lyons, L. R. (1980). Generation of large-scale regions of auroral currents, electric potentials, and precipitation by the convection electric field. *Journal of Geophysical Research*, *85*(A1), 17–24.
Lyons, L. R., Evans, D. S., & Lundin, R. (1079). An observed relation between magnetic field aligned electric fields and downward electron energy fluxes in the vicinity of auroral forms. *Journal of Geophysical Research*, *84*(A2), 457–461.
Lysak, R. L. (1981). Electron and ion acceleration by strong electrostatic turbulence. In S.-I. Akasofu, & J. R. Kan (Eds.), *Physics of auroral arc formation, geophysical monograph series 25* (pp. 444–450). Washington, DC: AGU
Lysak, R. L. (1985). Auroral electrodynamics with current and voltage generators. *Journal of Geophysical Research*, *90*, 4178
Lysak, R. L. (1990). Electrodynamic coupling of the magnetosphere and ionosphere. *Space Science Reviews*, *52*, 33–87.
Lysak, R. L., & Dum, C. T. (1983). Dynamics of magnetosphere- ionosphere coupling including turbulent transport. *Journal of Geophysical Research*, *88*, 365–380.
Marioka, A., Miyoshi, Y., Miyashita, Y., Kasaba, Y., Misawa, H., TsuchiyaKataoka, F. R., et al. (2010). *Journal of Geophysical Research*, *115*, A11213. https://doi.org/10.1029/JA015361
Marklund, G. T., Blomberg, L., Fälthammar, C.-G, & Lindqvist, P.-A. (1994). On intense diverging electric fields associated with black aurora. *Geophysical Research Letters*, *21*, 1859–1862. https://doi.org/10.1029/94GL00194
McFadden, J. P., Carlson, C. W., & Boehm, M. H. (1990). Structure of an energetic narrow discrete arc. *Journal of Geophysical Research*, *95*(A5), 6533–6547.
McFadden, J. P., Carlson, C. W., & Ergun, R. E. (1999). Microstructure of the auroral acceleration region as observed by FAST. *Journal of Geophysical Research*, *104*(A7), 14453–14480.
McIlwain, C. (1960). Direct measurement of particles producing visible aurora. *Journal of Geophysical Research*, *65*, 3681
Mizera, P. F., Gorney, D. J., & Fennell, J. F. (1982). Experimental verification of an S-shaped potential structure. *Journal of Geophysical Research*, *87*(A3), 1535
Mozer, F. S., Carlson, C. W., Hudson, M. K., Torbert, R. B., Parady, B., & Yatteau, J. (1977). Observations of paired electrostatic shocks in the polar magnetosphere. *Physical Review Letters*, *38*(6), 292–295.
Mozer, F. S., Cattell, C. A., Hudson, M. K., Lysak, R. L., Temerin, M., & Torbert, R. B. (1980). Satellite measurements and theories of low altitude auroral particle acceleration. *Space Science Reviews*, *27*, 155
Mozer, F. S., & Hull, A. (2001). Origin and geometry of upward parallel electric fields in the auroral acceleration region. *Journal of Geophysical Research*, *106*(A4), 5763–5778.
Mozer, F. S., & Kletzing, C. A. (1998). Direct observation of large, quasi-static, parallel electric fields in the auroral acceleration region. *Journal of Geophysical Research*, *25*(10), 1629–1632.
Otto, A., & Birk, G. T. (1993). Formation of thin auroral arcs by current striation. *Geophysical Research Letters*, *20*, 2833–2836. https://doi.org/10.1029/93GL02492
Partamies, N., Donovan, E., & Knudsen, D. (2008). Statistical study of inverted-V structures in FAST data. *Annales Geophysicae*, *26*, 1439–1449.
Sato, T. (1978). A theory of auroral arcs. *Journal of Geophysical Research*, *83*(A3), 1042–1048.
Shebalin, J. V., Mathaeus, W. H., & Montgomery, D. (1983), Anisotropy in MHD turbulence due to a mean magnetic field, *Journal of Plasma Physics 29*(3), 525–547.
Shelley, E. G., Sharp, R. D., & Johnson, R. G. (1976). Satellite observation of an ionospheric acceleration mechanism. *Geophysical Research Letters*, *3*, 654
Swift, D. W. (1975). On the formation of auroral arcs and acceleration of auroral electrons. *Journal of Geophysical Research*, *80*(16), 2096–2108.
Swift, D. W. (1979). An equipotential model for auroral arcs: The theory of two-dimensional electrostatic shocks. *Journal of Geophysical Research*, *84*, 6427
Zhou, Ye, Matthaeus, W. H., & Dmitruk, P. (2004). Colloquium: Magnetohydrodynamic turbulence and time scales in astrophysical and space plasmas. *Reviews of Modern Physics*, *76*, 1015–1035.